Journal of Fluids and Structures (2002) **16**(2), 213–227
doi:10.1006/jfls.2001.0412, available online at http://www.idealibrary.com on IDEAL®

EXPERIMENTAL STUDY ON LARGE-AMPLITUDE VIBRATIONS OF WATER-FILLED CIRCULAR CYLINDRICAL SHELLS

M. Amabili, R. Garziera and A. Negri

Dipartimento di Ingegneria Industriale, Università di Parma
Parco Area delle Scienze 181/A, Parma I - 43100, Italy

(Received 14 April 2000, and in final form 1 May 2001)

The response of two water-filled circular cylindrical shells made of steel to a harmonic excitation has been experimentally investigated in the neighbourhood of the fundamental mode. The boundary conditions at the shell edges approximate simple supports. The shell ends are closed by rubber disks to approximate a boundary condition of zero pressure for the water contained. Experimental results show a softening-type nonlinearity of about 4% for a vibration amplitude equal to twice the shell thickness. The travelling wave response around the shell has not been observed as a consequence of imperfections in the test specimens. Those imperfections separate the natural frequency of the two virtually identical (but rotated by $\pi/2n$, where n is the number of circumferential waves) fundamental modes. Experimental data agree well with the theoretical results obtained by using the model recently developed by Amabili, Pellicano and Païdoussis.

1. INTRODUCTION

The large-amplitude vibrations of circular cylindrical shells have interested many researchers in the last 40 years, as a consequence of the widespread applications in engineering. Many theoretical studies have been performed; however, not many experimental studies are available. The main reason for this, as pointed out by Evensen (1999) in a recent *Letter to the Editor*, is that nonlinear effects in shells occur in a very small frequency range and measurement is extremely difficult. However, Amabili, Pellicano and Païdoussis (1998, 2000*a*), Chiba (1993*a–c*) and Gonçalves & Batista (1988) have shown that a liquid-filled shell exhibits a much stronger softening behaviour than the same empty shell. This fact is important for applications and it also facilitates experimental measurements.

For a periodic excitation applied to the circular cylindrical shell, we expect a standing mode, symmetrical with respect to the point of application, in the case of linear vibrations. This symmetrical standing mode is called the *driven mode*. For large-amplitude vibrations, circumferentially travelling waves have been observed in the response of the shell. They can be described as the movement of the nodal lines of the driven mode. The travelling wave appears when a second standing mode, the orientation of which is at $\pi/(2n)$ (where n is the number of nodal diameters) with respect to the previous one, is added to the driven mode. This second mode is called the *companion mode*; it has the same modal shape and frequency as that of the driven mode. The presence of this second mode arises because of the axial symmetry of the shell and is due to the nonlinear coupling.

An extensive literature review of works on the nonlinear dynamics of shells *in vacuo* and filled with or surrounded by a quiescent fluid is given by Amabili *et al.* (1998). A fundamental paper describing the research work done in the former Soviet Union on nonlinear vibrations of shells has recently been written by Kubenko & Koval'chuk (1998). However, it is necessary to refer to some fundamental as well as some recent contributions. It is possible to attribute to Evensen (1967) and Dowell & Ventres (1968) the original idea of mode expansions of the flexural displacement involving the linear mode considered, the companion mode and an axisymmetric term; their intuition was supported by few available experimental results. The studies of Ginsberg (1973) and Chen & Babcock (1975) constitute fundamental contributions to the study of the influence of the companion mode on the nonlinear forced response of circular cylindrical shells. Ginsberg (1973) employed an expansion involving ideally all the linear modes plus an axial displacement to satisfy the nonlinear boundary conditions. He found that the fundamental terms in the expansion of the radial displacement are the excited modes, the companion mode, all the axisymmetric modes with an odd number of axial half-waves, plus the modes with a circumferential wavenumber twice that being excited. Chen & Babcock (1975) used a sophisticated mode expansion, including boundary layer terms, in order to satisfy the nonlinear boundary conditions. Gonçalves & Batista (1988) and Amabili *et al.* (1998) studied the response of fluid-filled shells. In particular, Gonçalves & Batista (1988) neglected the companion mode participation, the importance of which in the nonlinear response was investigated by Amabili *et al.* (1998). In a recent series of papers, Amabili *et al.* (1999*a*, *b*, 2000*a*, *b*) systematically studied the nonlinear dynamics and vibrations of circular cylindrical shells with and without quiescent or flowing fluid. Donnell's nonlinear shallow-shell theory was used; boundary conditions and continuity of circumferential displacements were satisfied. Potential flow was used to describe the fluid–structure interaction. In the present study, the theoretical model developed in this last series of studies is used to compare theoretical and experimental results.

Few experimental studies on large-amplitude vibrations of empty and fluid-filled shells are available. Experiments on empty shells have been reported by Olson (1965), Kaña *et al.* (1966), Kaña (1966), Matsuzaki & Kobayashi (1969), Chen & Babcock (1975), Chiba (1993*b*) and Koval'chuk & Lakiza (1995). In particular, Olson (1965), Kaña *et al.* (1966), Kaña (1966) and Chen & Babcock (1975) tested ring-supported shells by using an acoustic excitation that does not allow controlling the excitation pressure transmitted to the shell. Olson (1965) observed a slight nonlinearity of the softening type in the experimental response of a thin seamless shell made of copper; the measured change in vibration frequency was about 0·75% for a vibration amplitude equal to 2·5 times the shell thickness. He also found a double-frequency nodal contraction that is the justification for the mode expansion involving an axisymmetric term. Kaña *et al.* (1966; see also Kaña 1966) also found experimentally a weak softening-type response for a thin, simply supported, circular cylindrical shell. Matsuzaki & Kobayashi (1969) carried out experiments on clamped shells; no information was given on the excitation control. Chiba (1993*b*) tested two cantilevered circular cylindrical shells made of polyester sheet and used an accelerometer to control the excitation amplitude. This excitation control is different from the classical force control in the measurement of the shell response; however, the main aim of this work was to measure the backbone curve, indicating the nonlinear resonant characteristic. Chiba (1993*b*) found that almost all responses have a softening nonlinearity. He observed that for modes with the same axial wavenumber, the weakest nonlinearity (as usual, of softening type) can be attributed to the mode having the lowest natural frequency. He also found that shorter shells have a larger softening nonlinearity than longer ones. Travelling wave modes were also observed.

Koval'chuk & Lakiza (1995) experimentally investigated forced vibrations of large amplitude in empty fibreglass shells of revolution. Boundary conditions at the shell bottom simulated a clamped end, while the top was free (cantilevered shell). One of the tested shells was circular cylindrical. A weak softening-type nonlinearity was found, excluding the beam-bending mode, for which a hardening nonlinearity was measured. Detailed responses for three different excitation levels were obtained for the mode with four circumferential waves (second mode of the shell). No closed-loop control to maintain the force excitation constant was used. Travelling wave response was observed around the shell resonance, as well as the expected weak softening-type nonlinearity.

Experimental results on large-amplitude vibrations of empty and partially filled circular cylindrical shells were reported by Kaña (1966). He collected results published in previous papers (Kaña *et al.* 1966; Abramson & Kaña 1966) and reports. In most studies, water was used as the contained liquid, with a free surface. Simply supported and cantilevered shells subjected to radial and longitudinal excitations were tested. In particular, simply supported shells completely filled with water, presenting a free surface with sloshing waves, had a reduction of its natural frequency of about 0·4% for a vibration amplitude equal to one-third of the shell thickness under a radial excitation. This nonlinear behaviour was stronger than that measured for the same empty shell. It must be observed that for the completely filled shell, the height of free-surface waves was not very pronounced because the free surface was at an axial node of shell vibration. When the free surface was in the vicinity of an axial antinode of shell vibration, a much stronger nonlinearity of softening type was observed of the order of about 1·6% for a vibration amplitude of 0·29 times the shell thickness. This phenomenon was attributed to the nonlinear coupling between sloshing (free-surface oscillations) and bulging (shell oscillations) modes. High-frequency, large-amplitude free-surface waves were also excited by a relatively small vibration amplitude of the shell. Similar results were observed for cantilevered shells.

Ramachandran (1979) presented an experimental result showing a softening-type nonlinearity for a shell submerged in water. Sivak & Telalov (1991) obtained experimental results for the backbone curve (relative to free vibrations) on a vertical circular cylindrical shell made of titanium alloy in contact with water having a free surface. The experiments were performed with the shell partially filled and partially submerged in water with radial excitation. The experimental boundary conditions simulated a clamped shell. The backbone curve was obtained by using the phase method. Most of the experiments indicated a softening-type nonlinearity; however, the completely filled shell shows a hardening-type nonlinearity, an effect increasing with the circumferential wavenumber. It must be observed that the weight of the liquid can introduce a significant stress in thin shells, and this effect can give rise to a hardening behaviour in the experiments. Moreover, the phase method is not as accurate as is the measure of the complete response curve. It seems more reasonable that water-filled shells not subjected to gravity should show a softening nonlinearity, as experimentally observed by other researchers.

Chiba (1993*c*) studied experimentally large-amplitude vibrations of two vertical cantilevered circular cylindrical shells made of polyester sheet, partially filled to four different levels of water; the water had a free surface. Both backbone curves and system responses were reported. As observed for the same empty shells, the nonlinearity increased with the number of axial waves. He also found that shorter tanks have a larger softening nonlinearity than longer ones, as *in vacuo*. The tank with a lower liquid height had a greater softening nonlinearity than the tank with a higher liquid level. Travelling wave modes and coupling between two bulging modes (and between two sloshing modes) were also observed. Chiba (1993*c*) also investigated experimentally the effect of a thin film floating on the free surface and the behaviour of the free surface. Large-amplitude vibrations of two vertical clamped circular cylindrical shells, partially filled to four different levels of water were also studied by Chiba (1993*a*). In this case as well, the responses displayed a general softening nonlinearity.

The shells tested showed a larger nonlinearity when partially filled, as compared to the empty and completely filled cases. All the experiments were performed by controlling the excitation input with an accelerometer. The experiments of Chiba (1993*a–c*) gave a maximum softening nonlinearity of 6% for empty shells and of 8% for partially filled shells.

In the present study, experiments have been performed on circular cylindrical shells made of steel and completely filled with water. The shells tested had geometric imperfections: a longitudinal seam and sensor masses. Those imperfections separated the natural frequency of the driven and companion modes of a few Hz. For this reason, a travelling wave response has not been observed in the experiments. The shell response has been measured by using accelerometers, both increasing and decreasing the excitation frequency. A control of the harmonic force input has been used. A comparison between the experimental data and the results of the theoretical model developed by Amabili *et al.* (1999*a*, *b*, 2000*a*, *b*) has been performed.

2. SUMMARY OF THE THEORETICAL MODEL USED

Attention is focused on a finite, simply supported, closed circular cylindrical shell of length L. A cylindrical coordinate system (O; x, r, θ) is chosen, with the origin O placed at the centre of one end of the shell. The displacements of points in the middle surface of the shell are denoted by u, v and w, in the axial, circumferential and radial directions, respectively. Using Donnell's nonlinear shallow-shell theory, the equation of motion for large-amplitude transverse vibrations of a very thin, circular cylindrical shell is given by (Amabili *et al.* 1999*a*)

$$D\nabla^4 w + ch\dot{w} + \rho h\ddot{w} = f - p + \frac{1}{R}\frac{\partial^2 F}{\partial x^2} + \left(\frac{\partial^2 F}{R^2\partial\theta^2}\frac{\partial^2 w}{\partial x^2} - 2\frac{\partial^2 F}{R\partial x\partial\theta}\frac{\partial^2 w}{R\partial x\partial\theta} + \frac{\partial^2 F}{\partial x^2}\frac{\partial^2 w}{R^2\partial\theta^2}\right), \tag{1}$$

where $D = Eh^3/[12(1-\nu^2)]$ is the flexural rigidity, E is Young's modulus, ν is the Poisson ratio, h is the shell thickness, R is the mean shell radius, ρ is the mass density of the shell, c (kg m^{-3} s^{-1}) is the damping coefficient, and f and p are the radial pressures applied to the surface of the shell as a consequence of the external excitation and of the contained fluid, respectively. In the case of point-force excitation, f is given by

$$f = (\tilde{f}/R)\delta(\theta - \tilde{\theta})\delta(x - \tilde{x})\cos(\omega t), \tag{2}$$

where δ is the Dirac delta function, $\tilde{f}$ gives the force amplitude, $\tilde{\theta}$ and $\tilde{x}$ give the angular and axial positions of the point of application of the force, respectively. Here, the point excitation is located at $\tilde{\theta} = 0$, $\tilde{x} = L/2$. The radial deflection w is positive inward, and $\dot{w} = (\partial w/\partial t)$, $\ddot{w} = (\partial^2 w/\partial t^2)$; F is the in-plane stress function, given by (Amabili *et al.* 1999*a*)

$$\frac{1}{Eh}\nabla^4 F = -\frac{1}{R}\frac{\partial^2 w}{\partial x^2} + \left[\left(\frac{\partial^2 w}{R\partial x\partial\theta}\right)^2 - \frac{\partial^2 w}{\partial x^2}\frac{\partial^2 w}{R^2\partial\theta^2}\right]. \tag{3}$$

In equations (1) and (3), the biharmonic operator is defined as $\nabla^4 = [\partial^2/\partial x^2 + \partial^2/(R^2\partial\theta^2)]^2$. Donnell's nonlinear shallow-shell equations are accurate only for modes of high circumferential wavenumber n; specifically, $1/n^2 \ll 1$ must be satisfied, requiring $n \geq 5$ to have fairly good accuracy.

The following expansion of the flexural deformation w is used:

$$w(x, \theta, t) = \sum_{k=1}^{2} [A_{m,kn}(t)\cos(kn\theta) + B_{m,kn}(t)\sin(kn\theta)] \times \sin(m\pi x/L) + \sum_{m=1}^{2} A_{(2m-1),0}(t)\sin(\lambda_{(2m-1)}x), \tag{4}$$

where $\lambda_m = m\pi/L$, $A_{m,n}(t)$, $B_{m,n}(t)$ and $A_{m,0}(t)$ are unknown functions of time t and are used as generalized coordinates; m is the number of axial half-waves. The mode expansion given in equation (4) has been proved to give accurate results for shell response of modes with one longitudinal half-wave (Amabili *et al.* 1999*b*, 2000*a*). The mode associated with the generalized coordinate $A_{m,n}(t)$ is directly driven by the excitation and is called *driven mode*. The mode associated with the generalized coordinate $B_{m,n}(t)$ has the same shape and frequency but is angularly rotated by $\pi/(2n)$. This mode is assumed to have a node at the point-force input and is therefore called *companion mode*; its presence is not predicted by linear theory.

Equation (4) satisfies the boundary conditions

$$w = 0, \tag{5a}$$

$$M_x = -D\{(\partial^2 w/\partial x^2) + \nu[\partial^2 w/(R^2 \partial\theta^2)]\} = 0 \quad \text{at } x = 0, L; \tag{5b}$$

where M_x is the bending moment per unit length. The other boundary conditions for a classical simply supported shell are

$$N_x = 0 \quad \text{at } x = 0, L \qquad \text{and } v = 0 \quad \text{at } x = 0, L; \tag{6a, b}$$

moreover, u, v and w must be continuous in θ. Equations 6(a, b) are satisfied on the average at the shell ends but the continuity of the circumferential displacement v is satisfied exactly. Potential flow theory was used to describe the fluid–structure interaction. All details of the solution and the final equations are given by Amabili *et al.* (1999*a*, *b*, 2000*a*, *b*) for shells with and without flow.

3. EXPERIMENTAL SET-UP

Tests were conducted on two commercial, identical circular cylindrical tanks made of steel and having a longitudinal seam weld. The first specimen is labelled "α" and the second "β". The flat, steel end-plates of the tanks were mostly removed, leaving only an annular part, 15 mm wide, to approximate the simply supported boundary condition of the shell; rubber discs 1 mm thick were glued to these annular end-plates. The tanks were filled with water. The zero-pressure fluid boundary condition was well approximated by the flexible rubber disks at the shell ends. The dimensions and material properties of the system were approximately: $L = 246$ mm, $R = 86{\cdot}5$ mm, $h = 0{\cdot}23$ mm, $E = 1{\cdot}9 \times 10^{11}$ Pa, $\rho = 7850$ kg/m^3, $\rho_w = 1000$ kg/m^3 and $\nu = 0{\cdot}3$ (ρ_w is the mass density of water). The shells were suspended with elastic cables to a box-type frame. A photograph of one of the test-shells is given in Figure 1(a).

The shells were subjected to harmonic excitation in the spectral neighbourhood of the lowest natural frequency, corresponding to mode $n = 6$ and $m = 1$, and their response was investigated. The excitation was provided by an electrodynamic exciter (shaker), model LDS V406 with power amplifier LDS PA100E, connected to the shell by a stinger at $x = 118$ mm, i.e. close to $x = L/2$, for shell α, as shown in Figure 1(b), and at $x = 110$ mm for shell β. A piezoelectric force transducer, model B&K 8200, of mass 21 g, was screwed to a base of 3·5 g which was glued to the shell; the stinger was screwed to the force transducer

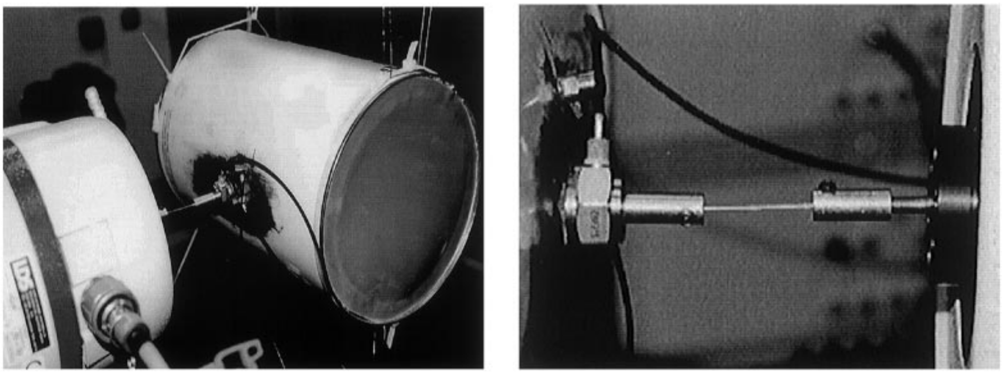

(a) (b)

Figure 1. Photograph of the tested shell being excited by the shaker. (a) Global view; (b) close-up of the stinger with the force transducer.

to measure the force transmitted. The shell response was measured by using two accelerometers, model B&K 4393, of mass 2·4 g, glued to the shell at $x = 96$ mm, i.e. $0{\cdot}39L$ $[\sin(\pi x/L) = 0{\cdot}94]$ for shell α, and at $x = 135$ mm, i.e. $0{\cdot}55\ L$ $[\sin(\pi x/L) = 0{\cdot}988]$, for shell β. The first accelerometer was placed at the same angular position as the stinger, to measure the driven mode [with a very small contribution of axisymmetric and $\cos(2n\theta)$ terms] and the second one at the same axial location with an angular distance of $\pi/12$, to capture the companion mode. The time responses were measured by using a Difa Scadas II front-end connected to an HP 715/80 workstation and using the software Ideas Test for signal processing and data analysis; the same front-end was used to generate the harmonic signal.

4. EXPERIMENTAL RESULTS

Results are reported separately for the test specimens α and β.

4.1. Specimen α

The fundamental frequency of the water-filled shell was measured to be 130·9 Hz, whereas the theoretical value, without the masses of transducers, is 134·7 Hz. The difference is attributed to imperfections in the test specimen and to the added mass of the sensors glued to the shell. The theoretical and measured (estimated by some FRFs) natural frequencies of the first three modes are given in Table 1. Modes have been identified by moving the accelerometers to find nodes at the resonance frequency and then measuring the distance between them. They can be recognized in the frequency response functions (FRFs) reported in Figure 2; these FRFs were obtained with the acceleration recorded by the two accelerometers and the force input measured by the sensor for a low excitation level by using a burst random signal.

The effect of sensors has also been theoretically investigated by using the method reported in Amabili (1996*a*); the frequency of the fundamental mode is lowered by at least 4 Hz and modes shapes are slightly distorted. Acceleration is expected to have different peak values on the antinodes as a consequence of the distortion of mode shapes. Moreover, this asymmetry of the structure causes a difference between the natural frequencies of the driven and companion modes, as experimentally verified.

TABLE 1

Theoretical and experimental natural frequencies for the water-filled test-shell α

Mode	Theoretical frequency (Hz)	Experimental frequency (Hz)
$n = 6$, $m = 1$ (driven)	134·7	130·9
$n = 6$, $m = 1$ (companion)	134·7	126·2
$n = 5$, $m = 1$	143·2	143·6
$n = 7$, $m = 1$	152·9	148·3

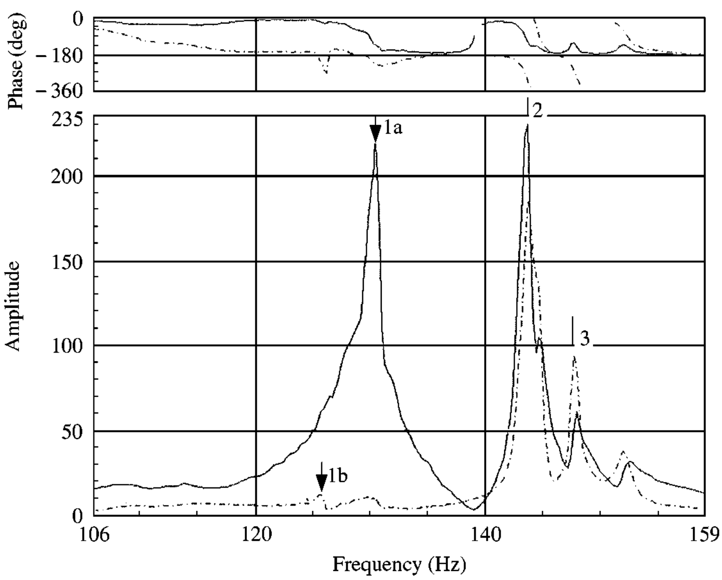

Figure 2. Measured FRFs of the water-filled shell α: ——, first accelerometer; – – –, second accelerometer. 1a, mode $n = 6$, $m = 1$; 1b, mode $n = 6$, $m = 1$ (companion); 2, mode $n = 5$, $m = 1$; 3, mode $n = 7$, $m = 1$.

Figure 3 shows the accelerations measured by the first accelerometer versus the excitation frequency, for two different force levels: 1·2 and 1·6 N. The excitation signal was controlled during tests in order to have a constant force measured by the force transducer. The measured acceleration was obtained as the peak value of the sinusoidal acceleration. Experiments were performed both increasing and decreasing the excitation frequency, and both curves are given in Figure 3; the hysteresis between the two is clearly visible. The jumps are indicated in the figure with dashed lines. A significant softening behaviour was observed. When the vibration amplitude was equal to the shell thickness, the peak of the response appeared for a frequency lower, by approximately 2%, than that at very low vibration amplitudes.

4.2. SPECIMEN β

The fundamental frequency of the water-filled shell was measured to be 131·2 Hz, whereas the theoretical value is 134·7 Hz. In this case also, the difference is attributed to imperfections in the test specimen and to the additional mass of the sensors glued to the shell. Theoretical and measured natural frequencies of the first three modes are reported in Table 2. They can be individuated in the FRFs reported in Figure 4.

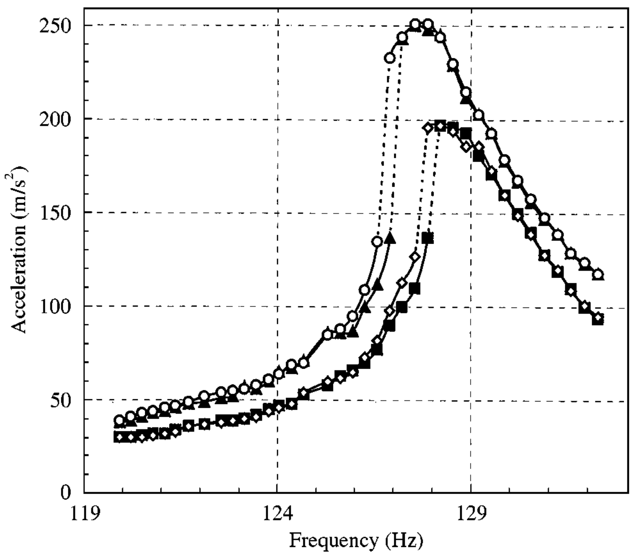

Figure 3. Experimentally measured frequency–response curves for the water-filled test shell α; first accelerometer: —■—, force level 1·2 N, increasing frequency; —◇—, force level 1·2 N, decreasing frequency; —▲—, force level 1·6 N, increasing frequency; —○—, force level 1·6 N, decreasing frequency.

TABLE 2

Theoretical and experimental natural frequencies for the water-filled test-shell β

Mode	Theoretical frequency (Hz)	Experimental frequency (Hz)
$n = 6$, $m = 1$ (driven)	134·7	131·2
$n = 6$, $m = 1$ (companion)	134·7	134·8
$n = 5$, $m = 1$	143·2	145·6
$n = 7$, $m = 1$	152·9	155·8

Figure 5 shows the accelerations measured by the first accelerometer versus the excitation frequency for the single force level 2·4 N. The measured acceleration was obtained as the peak value of the sinusoidal acceleration. Experiments were performed both increasing and decreasing the excitation frequency, and both curves are given in Figure 5; the hysteresis between the two is clearly visible. The jumps are indicated in the figure with dashed lines. A larger softening behaviour was observed in this case with respect to the case shown in Figure 3, corresponding to the increased vibration amplitude. A larger damping was also observed; this is attributed to the higher tension of the rubber disk in this specimen with respect to shell α.

The phase between the shell acceleration measured by the first accelerometer and the force input is given in Figure 6. It is important to note that the positive directions of force and acceleration transducers are opposite in the experimental set-up; therefore, the phase for excitation frequencies significantly lower than that for resonance is almost zero instead of the expected value π.

The time histories of the force and acceleration recorded by the two accelerometers are reported in Figures 7 and 8 for two different excitation frequencies. Figure 7 shows a very clear force input that is almost in-phase with the acceleration measured by the first

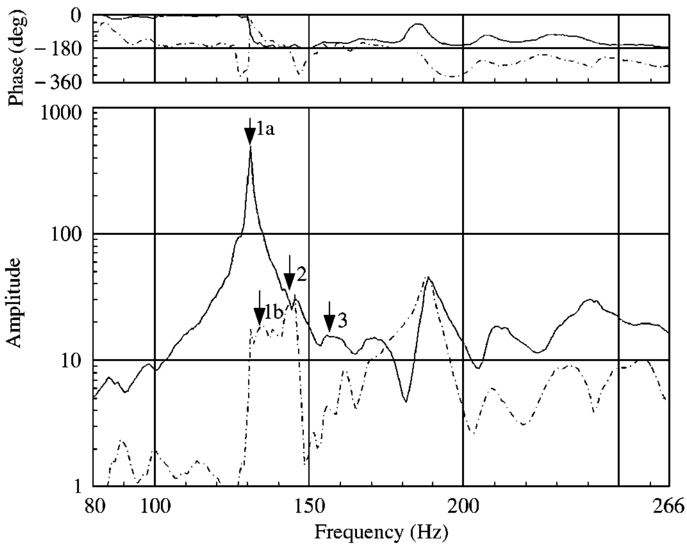

Figure 4. Measured FRFs of the water-filled shell β in semi-logarithmic scale: ——, first accelerometer; – – –, second accelerometer. 1a, mode $n = 6$, $m = 1$; 1b, mode $n = 6$, $m = 1$ (companion); 2, mode $n = 5$, $m = 1$; 3, mode $n = 7$, $m = 1$.

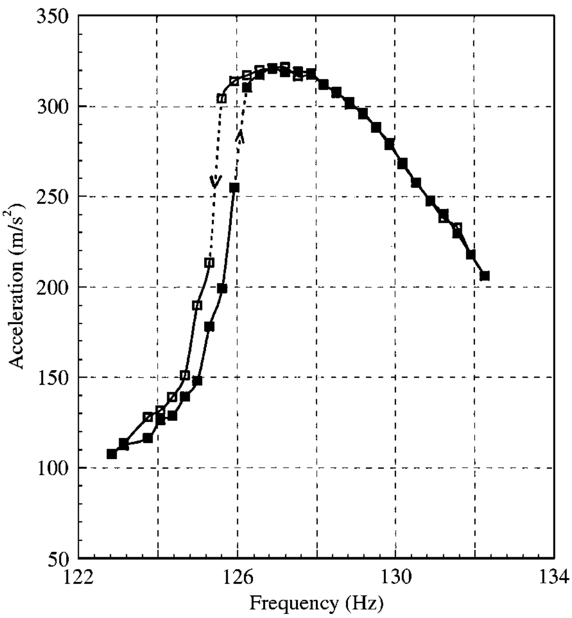

Figure 5. Experimentally measured frequency–response curves for the water-filled test-shell β; first accelerometer: —■—, force level 2·4 N, increasing frequency; —□—, force level 2·4 N, decreasing frequency.

accelerometer. The time histories have been recorded for an excitation frequency of 122·9 Hz, i.e., before the resonance. The acceleration measured by the second accelerometer shows a more complex behaviour that may be interpreted as a superposition of the double-frequency axisymmetric contraction (also called nodal contraction) of the shell and

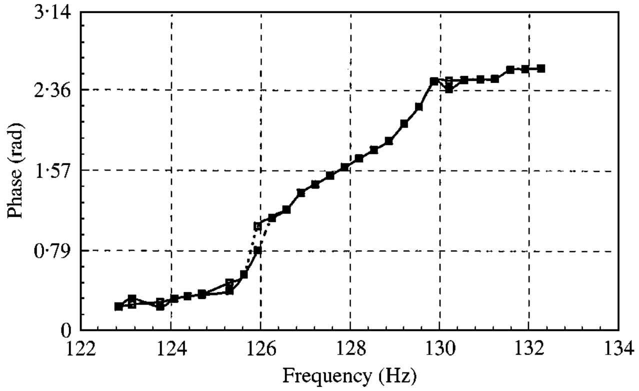

Figure 6. Experimentally measured phase between acceleration response and force input for the water-filled test-shell β; first accelerometer: —■—, force level 2·4 N, increasing frequency; —□—, force level 2·4 N, decreasing frequency.

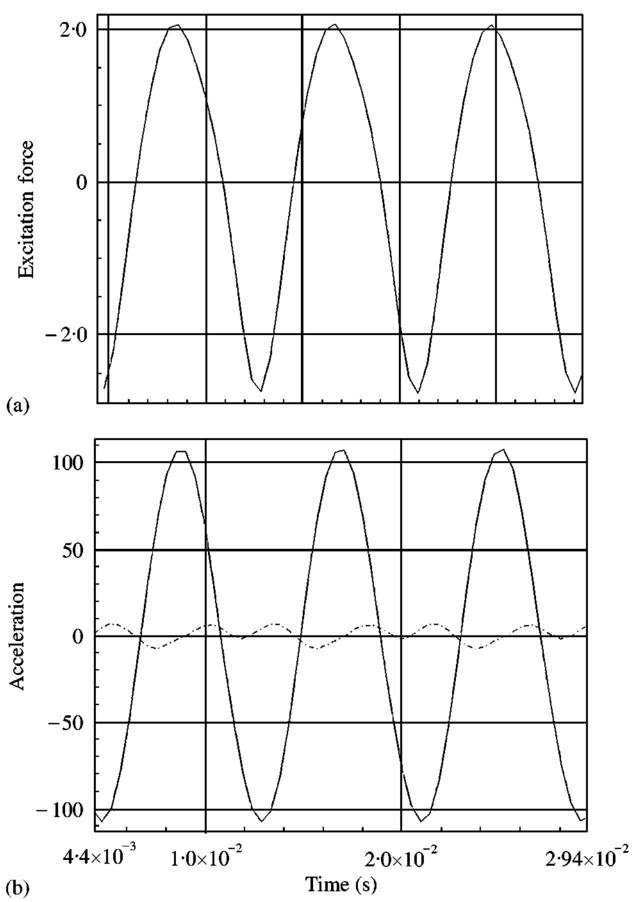

Figure 7. Time traces recorded for shell β for excitation frequency 122·9 Hz, increasing frequency. (a) Force transducer; (b) ——, first accelerometer; – – –, second accelerometer.

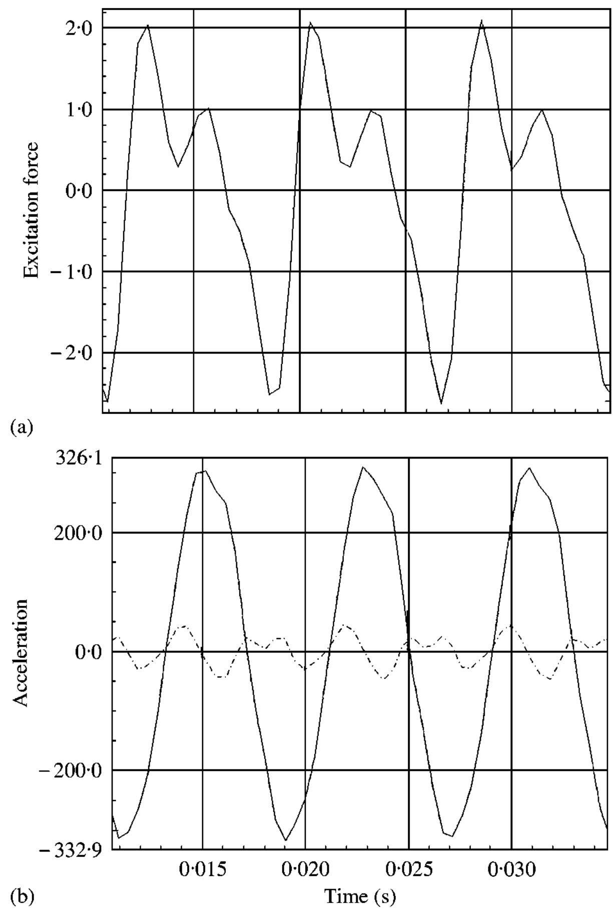

Figure 8. Time traces recorded for shell β for excitation frequency 126·26 Hz, increasing frequency. (a) Force transducer; (b) ——, first accelerometer; – – –, second accelerometer.

a movement due to a small excitation of the companion mode. In fact, the force excitation is actually distributed on an area of a few millimetres of radius; therefore, it can directly excite the companion mode, even with a force several times smaller than the one forcing the driven mode.

The time histories recorded for an excitation frequency of 126·26 Hz, measured by increasing the excitation frequency, are reported in Figure 8. The response of the system is the one just after the jump in Figure 5. The force input is distorted, especially for the compressive force. In general, a significant distortion of the force input has been observed for some points just after the jump, when increasing the excitation frequency, or just before the jump, when decreasing the frequency. These distortions increase with the vibration amplitude; therefore, the measurement of smaller vibration amplitudes, as done for specimen α, is easier and the results are more reliable. The acceleration measured by the first accelerometer is relatively clean. As in the previous case for a lower excitation frequency, the acceleration measured by the second accelerometer shows a behaviour that can also be interpreted as a superposition of the double-frequency axisymmetric contraction of the shell and a small participation of the companion mode. It is interesting to observe that the acceleration of the second accelerometer is almost zero where the signal of the first accelerometer has a maximum absolute value.

5. COMPARISON OF THEORETICAL AND EXPERIMENTAL RESULTS AND DISCUSSION

The measured accelerations have been converted to displacements, dividing them by the excitation circular frequency squared. These values have been compared to the theoretical curves. The theoretical results have been obtained by using the theory developed by Amabili *et al.* (1999*a*, *b*; 2000*a*, *b*) and summarized in Section 2. In particular, the effects of the hydrostatic pressure due to the water and the beam-bending of the shell due to its weight have been neglected in the theoretical model. The annular plates at the shell ends have been considered only as constraints for the shell, as well as the rubber disk. In fact, the rubber disks were so flexible that they were largely uncoupled from the shell resonance (the fundamental natural frequency was around 1 Hz); their contribution was mainly an additional damping.

The model is based on the expansion of the radial displacement of the shell given by equation (4). Therefore, the interaction among the driven mode (having n circumferential waves), modes having $2n$ circumferential waves, and axisymmetric modes was considered. However, the interaction with modes having a different number of circumferential waves, was neglected. This approximation is usually acceptable when the shell response is computed only in the neighbourhood of the resonance of the driven mode. When approaching a resonance or an antiresonance involving modes with a different number of circumferential waves, the model loses its accuracy.

A change of the linear frequency of the companion mode has been included in the model, to take into account imperfections. This change was equal to that measured experimentally. By introducing this change in frequency, the companion mode participation to large-amplitude vibrations of the driven mode has not been observed anymore in the theoretical results for the experimental excitation levels.

5.1. Specimen α

The shell displacements have been plotted in Figure 9, together with the theoretical responses without companion mode participation [practically coincident with $A_{1,n}(t)$ in this case], since the participation of the companion mode was nearly negligible in the experiments; the reason for this behaviour is explained as follows. The theoretical values are calculated at $x = 0{\cdot}39L$ (it is necessary to multiply the theoretical values at $x = 0{\cdot}5L$ by 0·94) in order to compare them with the experimental data. The damping used to produce the theoretical curves is $\zeta_{1,n} = 0{\cdot}011$, i.e., a damping ratio of 1·1%, which is in agreement with the experimental values obtained by Amabili (1996*b*) for vibrations of a water-filled circular cylindrical shell made of steel with thin end-plates. The experimental forces are smaller than the theoretical ones, because there are additional loads (sensors) on the shell at the force input.

The agreement between the theoretical curves and the experimental results is very good; in particular, it is excellent for the lowest curve. The experimental points on the right-hand part of Figure 9, for both forcing amplitudes, lie to the left of the theoretical curves. This may be explained by the presence of another mode, $n = 5$ and $m = 1$, which is very close in frequency to the fundamental mode investigated ($n = 6$, $m = 1$) in the shell tested, as shown in Table 1. Between the two modes an antiresonance has been experimentally detected; this is sufficiently close to the peak of the response of the fundamental mode to modify the

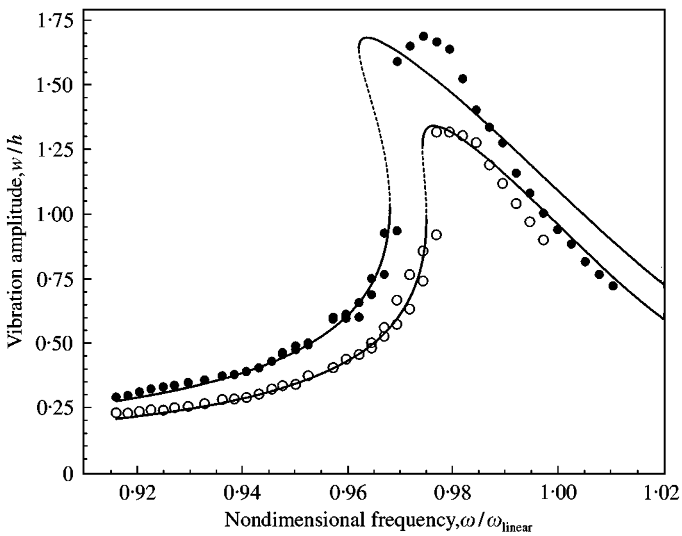

Figure 9. Frequency–response relationship at $x = 0{\cdot}39L$ for the water-filled test-shell α; driven mode: ●, experimental data, force level 1·2 N; ○, experimental data, force level 1·6 N; ——, stable theoretical solutions; – – –, unstable theoretical solutions.

experimental response (with at least a linear effect) on the right-hand part of Figure 9. In fact, it is important to clarify that the theoretical response does not take into account the interaction between the fundamental mode ($n = 6$, $m = 1$) and the additional mode ($n = 5$, $m = 1$).

The participation of the companion mode in the large-amplitude vibrations of the driven mode has been found to be negligible in the experiments. It has been observed experimentally that the companion mode has in fact a natural frequency approximately 3% lower than the driven mode, see Table 1, as a consequence of the test-shell not being perfectly axisymmetric due to manufacturing imperfections, the presence of the seam and the sensors attached to the shell. This difference between the natural frequency of the driven and companion modes is the reason for the almost negligible participation of the companion mode to vibrations of the driven mode around the resonance. In fact, the participation of the companion mode is due to one-to-one internal resonance between the natural frequency of the driven and companion modes. If the difference between the frequencies of driven and companion modes becomes too large, the internal resonance can disappear, at least for small force excitations.

5.2. Specimen β

Figure 10 gives theoretical versus experimental responses without the companion mode participation, since, for this case as well, the second accelerometer recorded only small oscillations of the companion mode, as shown in Figure 8. The damping used to produce the theoretical curves is $\zeta_{1,n} = 0{\cdot}015$, i.e., a damping ratio of 1·5%. The agreement between theoretical and experimental results is reasonable. In fact, it must be observed that the vibration amplitude in this case is quite large, the force input is largely distorted and a small participation of the companion mode has been observed. The latter decreases the softening behaviour of the driven mode response cutting it, as theoretically observed [e.g., Amabili *et al.* (1998, 1999*b*)].

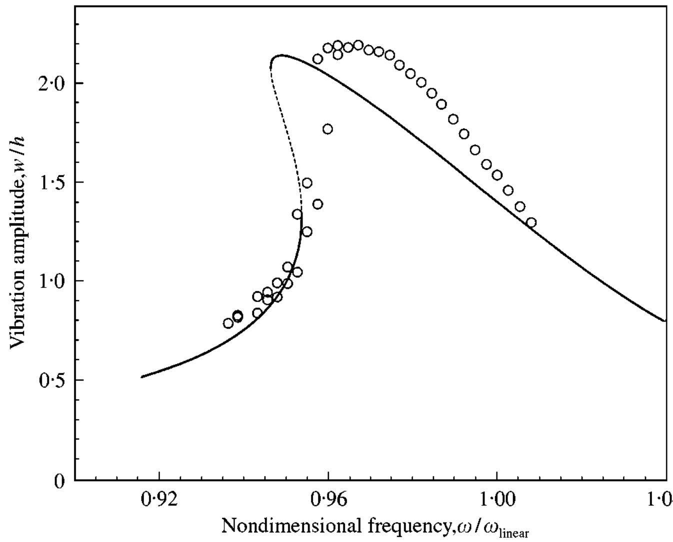

Figure 10. Frequency–response relationship at $x = 0{\cdot}55L$ for the water-filled test shell β; driven mode: ○, experimental data, force level 2·4 N; ——, stable theoretical solutions; - - -, unstable theoretical solutions.

6. CONCLUSIONS

The response of two water-filled circular cylindrical shells made of steel has been investigated in the neighbourhood of the fundamental mode ($n = 6$, $m = 1$). The boundary conditions at the shell edges approximate a simple support. The shell ends are closed by a rubber disk to approximate a boundary condition of zero pressure for the water contained.

Experimental results show a softening-type nonlinearity of approximately 4% for a vibration amplitude equal to twice the shell thickness. The travelling wave response around the shell has not been observed as a consequence of imperfections in the test specimens. Those imperfections separate the natural frequency of the two virtually identical (but rotated by $\pi/2n$, where n is the number of circumferential waves) fundamental modes. Experimental data agree well with the theoretical results obtained by using the model recently developed by Amabili *et al.* 1999*a*, b; 2000*a*, *b*).

ACKNOWLEDGEMENTS

This work was partially supported by a grant of the Italian Space Agency (ASI).

REFERENCES

Abramson, H. N. & Kaña, D. D. 1966 Some recent research on the vibrations of elastic shells containing liquids. In *Proceedings of the Symposium on the Theory of Shells*, pp. 253–310. University of Houston, U.S.A.

Amabili, M. 1996*a* Free vibration of a fluid-filled circular cylindrical shell with lumped masses attached, using the receptance method. *Shock and Vibration* **3,** 159–167.

Amabili, M. 1996b Free vibration of partially filled, horizontal cylindrical shells. *Journal of Sound and Vibration* **191,** 757–780.

AMABILI, M., PELLICANO, F. & PAÏDOUSSIS, M. P. 1998 Nonlinear vibrations of simply supported, circular cylindrical shells, coupled to quiescent fluid. *Journal of Fluids and Structures* **12,** 883–918.

AMABILI, M., PELLICANO, F. & PAÏDOUSSIS, M. P. 1999*a* Non-linear dynamics and stability of circular cylindrical shells containing flowing fluid. Part I: stability. *Journal of Sound and Vibration* **225,** 655–699.

AMABILI, M., PELLICANO, F. and PAÏDOUSSIS, M. P. 1999*b* Non-linear dynamics and stability of circular cylindrical shells containing flowing fluid. Part II: large amplitude vibrations without flow. *Journal of Sound and Vibration* **228,** 1103–1124.

AMABILI, M., PELLICANO, F. & PAÏDOUSSIS, M. P. 2000*a* Non-linear dynamics and stability of circular cylindrical shells containing flowing fluid. Part III: truncation effect without flow and experiments. *Journal of Sound and Vibration* **237,** 617–640.

AMABILI, M., PELLICANO, F. & PAÏDOUSSIS, M. P. 2000*b* Non-linear dynamics and stability of circular cylindrical shells containing flowing fluid. Part IV: large-amplitude vibrations with flow. *Journal of Sound and Vibration* **237,** 641–666.

CHEN, J. C. & BABCOCK, C. D. 1975 Nonlinear vibration of cylindrical shells. *AIAA Journal* **13,** 868–876.

CHIBA, M. 1993*a* Experimental studies on a nonlinear hydroelastic vibration of a clamped cylindrical tank partially filled with liquid. *ASME Journal of Pressure Vessel Technology* **115,** 381–388.

CHIBA, M. 1993*b* Non-linear hydroelastic vibration of a cantilever cylindrical tank. I. Experiment (empty case). *International Journal of Non-Linear Mechanics* **28,** 591–599.

CHIBA, M. 1993*c* Non-linear hydroelastic vibration of a cantilever cylindrical tank. II. Experiment (liquid-filled case). *International Journal of Non-Linear Mechanics* **28,** 601–612.

DOWELL, E. H. & VENTRES, C. S. 1968 Modal equations for the nonlinear flexural vibrations of a cylindrical shell. *International Journal of Solids and Structures* **4,** 975–991.

EVENSEN, D. A. 1967 Nonlinear flexural vibrations of thin-walled circular cylinders. NASA TN D–4090.

EVENSEN, D. A. 1999 Nonlinear vibrations of cylindrical shells—logical rationale. *Journal of Fluids and Structures* **13,** 161–164.

GINSBERG, J. H. 1973 Large amplitude forced vibrations of simply supported thin cylindrical shells. *Journal of Applied Mechanics* **40,** 471–477.

GONÇALVES, P. B. & BATISTA, R. C. 1988 Non-linear vibration analysis of fluid-filled cylindrical shells. *Journal of Sound and Vibration* **127,** 133–143.

KAÑA, D. D. 1966 Interaction between liquid propellants and the elastic structure. In *The Dynamic Behaviour of Liquids in Moving Containers* (ed. H. N. Abramson), pp. 303–352. NASA-SP-106, Washington, DC: Government Printing Office.

KAÑA, D. D., LINDHOLM, U. S. & ABRAMSON, H. N. 1966 Experimental study of liquid instability in a vibrating elastic tank. *Journal of Spacecraft and Rockets* **3,** 1183–1188.

KOVAL'CHUK, P. S. & LAKIZA, V. D. 1995 Experimental study of induced oscillations with large deflections of fiberglass shells of revolution. *International Applied Mechanics* **31,** 923–927.

KUBENKO, V. D. & KOVAL'CHUK, P. S. 1998 Nonlinear problems of the vibration of thin shells (review). *International Applied Mechanics* **34,** 703–728.

MATSUZAKI, Y. & KOBAYASHI, S. 1969 A theoretical and experimental study of the nonlinear flexural vibration of thin circular cylindrical shells with clamped ends. *Transactions of the Japan Society for Aeronautical and Space Sciences* **12,** 55–62.

OLSON, M. D. 1965 Some experimental observations on the nonlinear vibration of cylindrical shells. *AIAA Journal* **3,** 1775–1777.

RAMACHANDRAN, J. 1979 Non-linear vibrations of cylindrical shells of varying thickness in an incompressible fluid. *Journal of Sound and Vibration* **64,** 97–106.

SIVAK, V. F. & TELALOV, A. I. 1991 Experimental investigation of vibrations of a cylindrical shell in contact with a liquid. *Soviet Applied Mechanics* **27,** 484–488.